

Measuring the Thickness of the Human Cerebral Cortex from Magnetic Resonance Images

Bruce Fischl

*Nuclear Magnetic Resonance Center
Massachusetts Gen. Hosp/ Harvard Med. School
Bldg. 149, 13th St.
Charlestown, MA 02129
tel: 617 726 4879
fax: 617 726-7422
fischl@nmr.mgh.harvard.edu*

and

Anders M. Dale *

*Nuclear Magnetic Resonance Center
Massachusetts Gen. Hosp/ Harvard Med. School
Bldg. 149, 13th St.
Charlestown, MA 02129
tel: 617 724 8304
fax: 617 726-7422
dale@nmr.mgh.harvard.edu*

Keywords: Atrophy, thickness, morphometry, surface reconstruction, Huntington's, Alzheimer's, schizophrenia.

* Author to whom correspondence should be addressed.

***Abstract** - Accurate and automated methods for measuring the thickness of human cerebral cortex could provide powerful tools for diagnosing and studying a variety of neurodegenerative and psychiatric disorders. Manual methods for estimating cortical thickness from neuroimaging data are labor intensive, requiring several days of effort by a trained anatomist. Furthermore, the highly folded nature of the cortex is problematic for manual techniques, frequently resulting in measurement errors in regions in which the cortical surface is not perpendicular to any of the cardinal axes. As a consequence, it has been impractical to obtain accurate thickness estimates for the entire cortex in individual subjects, or group statistics for patient or control populations. Here, we present an automated method for accurately measuring the thickness of the cerebral cortex across the entire brain, and for generating cross-subject statistics in a coordinate system based on cortical anatomy. The inter-subject standard deviation of the thickness measures is shown to be less than 1/2mm, implying the ability to detect focal atrophy in small populations or even individual subjects. The reliability and accuracy of this new method are assessed via within-subject test-retest studies, as well as comparison of cross-subject regional thickness measures with published values.*

1. Introduction.

The human cerebral cortex is a highly folded sheet of neurons the thickness of which varies between 1 and 4.5 millimeters, with an overall average of approximately 2.5 mm [1-3]. Regional variations in the cortical thickness can be quite large. For example, Brodmann area 3 on the posterior bank of the central sulcus is among the thinnest of cortical regions, with an average thickness of less than 2 millimeters, while Brodmann area 4 on the anterior bank is one of the thickest regions, frequently exceeding 4 millimeters. Interestingly, the distribution of the thickness is not uniform by layer, nor is the variation in the thickness of the cortical layers proportional to the variation in the total thickness.

The thickness of the cortex is of great interest in both normal development as well as a wide variety of neurodegenerative and psychiatric disorders. Changes in the gray matter that makes up the cortical sheet are manifested in normal aging [4, 5], Alzheimer's disease [4-10] and other dementias [11], Huntington's disease [12, 13], corticobasal degeneration [14], ALS [15], as well as schizophrenia [16-19]. The cortical thinning is frequently regionally specific, and the progress of the atrophy can therefore reveal much about the evolution and causative factors of a disease. Moreover, longitudinal studies of cortical atrophy are potentially of great utility in assessing the efficacy of a wide variety of treatments.

To date, few studies have been completed comparing the thickness of the cortical ribbon in large patient and age-matched normal subject populations. In large part this has been due to the complexity of the process of accurately measuring the cortical thickness on the sub-millimeter scale. For example, a complete labeling of a human brain from a high-resolution T1-weighted MRI scan can take a trained anatomist days to complete, and even this labor-intensive procedure only allows the measurement of cortical *volume*, not cortical *thickness*. This is because the thickness of the cortex is a property that can only be properly measured if the location and orientation of the gray/white and pial surfaces are both known. In spatially localized cases in which the image plane is orthogonal to the cortical surface throughout a region of interest, the measurement of thickness can be accomplished from slice data [20]. More typically however, cortical thickness measurements are obtained for spatially localized regions during post-mortem studies.

The difficulty of properly measuring the thickness of the cortex without explicit representations of both the gray/white and pial surfaces is illustrated in Figure 1 in Section 3, which shows coronal and axial slices through a T1-weighted MRI volume. Measuring the thickness from the coronal slice at the point indicated by the green cross would result in an estimate in excess of 1 cm. Examining the other view reveals that this is a dramatic overestimation, resulting from the fact that the surface is locally parallel to the coronal slice. The use of multiple orthogonal views in this fashion can reduce the degree of inaccuracy, as one can choose the slice plane that is closest to being perpendicular to the surface. Nevertheless, measuring the thickness of the cortex from slice data will always result in overestimates,

unless the cortical surface happens to be orthogonal to one of the viewing planes. In general, the true value of the thickness over the entire cortex cannot be accurately determined in this way, as the cortex contains many folds that are not aligned with any of the cardinal axes along which slice data is typically viewed. Thus, while thickness and/or volume measurements derived from slice data may suffice to detect gross changes in the cortex; they do not provide the sub-millimeter precision necessary to characterize the location and progression of subtle cortical atrophy. This is of particular importance, as detecting regionally specific cortical atrophy associated with the early stages of diseases such as Alzheimer's or Huntington's requires this type of precision, and accurately characterizing the early stages of degeneration may be critical to a deeper understanding of the causative factors in the disorders.

In order to address this need, we have developed a technique for automatically measuring the thickness of the gray matter of the human cerebral cortex. The measurement of the thickness is enabled by a procedure for generating highly accurate models of both the gray/white and pial surfaces. The distance between these two surfaces then gives the thickness of the cortical gray matter at any point. In conjunction with automated surface reconstruction [21-24] and high-resolution surface averaging techniques [25], the measurement of cortical thickness with sub-millimeter accuracy facilitates the use of powerful statistical methods in the investigation of neurodegeneration and recovery.

2. Methods.

Due to limitations on the resolution of MR imaging, it is difficult to directly compute the location of the pial surface [21]. Instead, we construct an estimate of the gray/white boundary by classifying all white matter voxels in an MRI volume. The surface of the connected white matter voxels is then refined to obtain sub-voxel accuracy in the representation of the gray/white boundary, and subsequently deformed outward to find the pial surface, as described in [22].

The basic technique described previously has been extended in a number of ways, and is similar in spirit to many deformable template algorithms in the computer vision and medical image processing literature [26-33]. First, we employ a multi-scale analysis, similar to the type described in [34], in order

to make the detection of the gray/white and pial boundaries less sensitive to noise. In addition, since the cortex itself is smooth at the spatial scale of a few millimeters (except in rare pathologies), we constrain the surface representation to be smooth in a similar manner. The machine vision and image processing research communities have developed many techniques for constraining an evolving curve or surface to be smooth, typically involving some form of minimization of the mean or the Gaussian curvature [27, 35, 36]. This is problematic for generating a surface that faithfully reflects the gray/white or pial surface, as there are highly curved regions at the fundi of sulci and the crowns of gyri. A smoothness constraint that seeks to minimize curvature will therefore result in surfaces that are inaccurate in these regions.

In order to reduce this source of error, we compute the curvature of patches of the surface, then alter the surface representation so that the local surface has this curvature at the finest (i.e. mm) scale as well. This technique produces a surface that is second-order smooth (i.e. has a continuous second derivative), in contrast to the curvature-reduction techniques, which attempt to generate a surface whose second derivative is zero. In localized regions in which the pial surface cannot be directly resolved, the smoothness constraint allows the surface to be accurately extended into ambiguous areas. In more extensive such regions, a self-intersection constraint placed on the evolving surface causes it to settle at approximately the midpoint of the sulcus¹.

It is important to note that, given a smooth underlying (true) cortical surface, the accuracy of this procedure is not directly limited by the voxel dimensions of the MRI data used to generate the cortical model. Assuming that the radius of curvature of the surface as well as the thickness of the tissue classes is greater than the size of the voxels, and assuming sufficient contrast-to-noise exists between the tissue classes, interpolation can be used to achieve sub-voxel accuracy.²

The surface deformation is implemented using gradient descent with momentum [37]. In order to prevent the surface from intersecting itself, a spatial lookup table in conjunction with fast triangle-triangle intersection code [38] is employed, resulting in computational complexity that is linear in the number of vertices in the surface representation. Specifically, if the movement of the k^{th} vertex results in

an intersection, the size of the movement of that vertex is reduced until the self-intersection no longer occurs. The entire procedure is carried out in a multi-scale manner, with the target intensity calculation using derivative information computed from images smoothed with a Gaussian kernel of a given standard deviation. The numerical integration continues until the error functional asymptotes. The standard deviation of the smoothing kernel is then decreased, the target intensities are recomputed, and the integration is repeated, until a predefined minimum scale is reached.

The numerical integration was carried out at 4 decreasing scales for the smoothing kernel ($\sigma=2$ mm, $\sigma=1$ mm, $\sigma=0.5$ mm, $\sigma=0.25$ mm), with the integration proceeding at each scale until the error functional decreased by less than 1%. The resulting procedure required approximately 5 hours to generate the gray/white and pial surfaces and thickness measurements on a 550 MHz Pentium III, with the majority of the computational complexity attributable to the self-intersection checking. Both the self-intersection code and the actual measurement of the cortical thickness employ a spatial lookup table in order to obtain $O(n)$ computational complexity, as opposed to the $O(n^2)$ that would be required to search the entire surface for self-intersection, or to find the point on one surface that is closest to a given point on the other. The thickness is computed as the average of this distance measured from each surface to the other.

3. Results.

In order to validate the thickness measurements, we computed the thickness of the cortical gray matter for the left hemisphere of 30 subjects (17 male, 13 female, ages 20-37). Two and three-dimensional examples of the results of the deformation process are given in Figure 1 and Figure 2 respectively, while Figure 3 gives a histogram of the distribution of thicknesses across the cortical surface of a representative subject. Note that the vast majority of the thickness measurements (over 99%) fall within the known bounds of 1 and 4.5 mm.

¹ Regions in which the border between opposing banks cannot be resolved, and whose thickness is asymmetric will of course then be inaccurate.

² All intensity values and intensity gradients are sampled from the volume using trilinear interpolation.

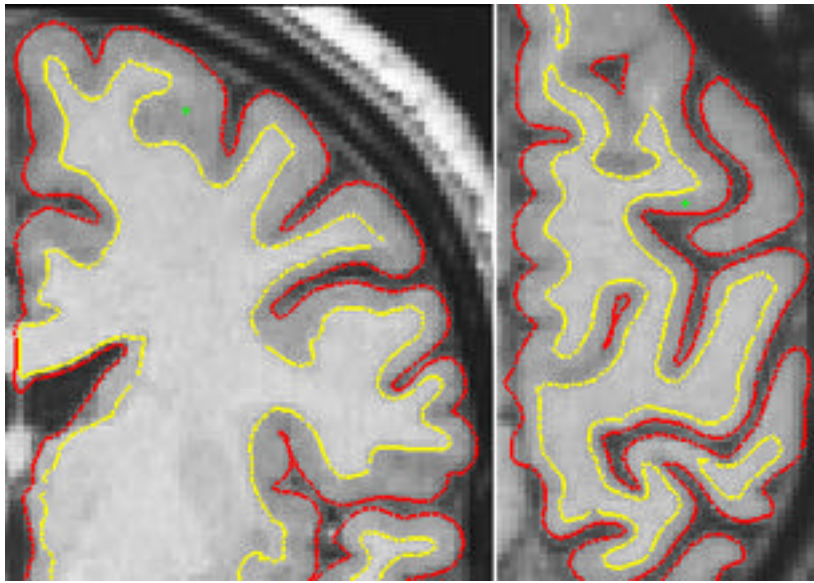


Figure 1. Coronal (left) and horizontal (right) slices of the left hemisphere with gray/white (yellow) and pial surfaces (red) overlaid. The green crosses indicate a point at which using only the coronal view would result in a dramatic overestimation of the thickness of the cortex.

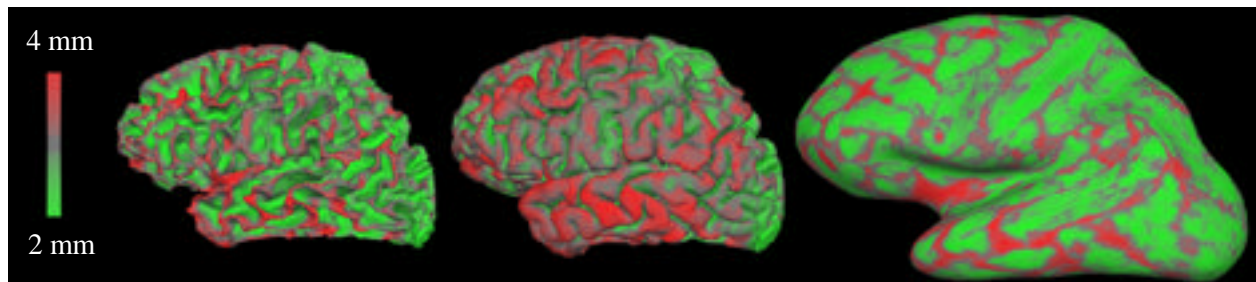


Figure 2. Lateral views of the gray/white (left) pial (center) and inflated (right) surface representations with cortical thickness measurements overlaid in a red/green color scale.

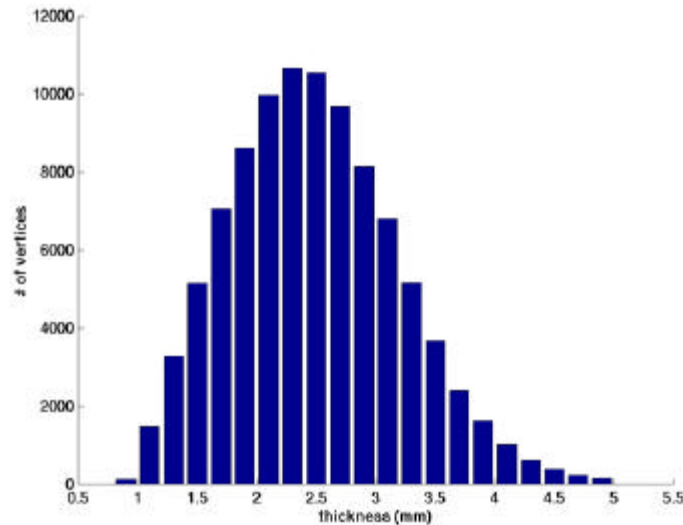


Figure 3. Histogram of thickness values in cortical regions of the subject shown in Figure 2. Over 99% of the surface is between 1 and 4.5 mm thick.

The individual thickness estimates from the results of this analysis were then combined across the 30 subjects using a high-resolution surface-based averaging technique that aligns cortical folding patterns [25]. The results of this procedure, shown in Figure 4, reveals that, consistent with published findings [2], the crowns of gyri are thicker than the fundi of sulci, and that sensory areas are among the thinnest in cortex. More specifically, we find that gyral regions have an average thickness of 2.7 ± 0.3 mm, versus 2.2 ± 0.3 mm for sulcal regions.³

An illustration of the variability of these results across the cortex is given in Figure 5, which shows the spatial distribution of the cross-subject standard deviations of the thickness measurements. As can be seen, the measurements are quite consistent across subjects, with a standard deviation of less than $\frac{1}{2}$ mm over much of cortex, with a mean of 0.54 mm. Applying a small surface-based Gaussian blurring kernel ($\sigma=7$ mm) reduced the standard deviation to 0.32 mm, indicating the auto-correlation of the noise falls off quite sharply with distance. One further point to note is that the majority of the variance is localized in association areas: anterior ventral temporal and prefrontal cortices, which are among the thickest of cortical regions.

³ Across the 30 subjects, we find that approximately 90% of the cortex maps gyral/sulcal patterns consistently across individuals. That is, a patch of cortex that is clearly gyral (sulcal) in one individual has a 90% chance of mapping to

In order to assess the portion of this variability attributable to measurement noise as opposed to true inter-subject differences, we performed two test-retest experiments. In the first, we scanned the same subject in two different sessions and reconstructed surface models for each, aligning them with the group average. The mean inter-session standard deviation of these thickness measures was found to be 0.25 mm. Applying the surface-based blurring kernel reduced the variability to 0.1 mm. Next, in order to assess the robustness of the technique to the varying contrast properties of different pulse sequences, we scanned the same subject on two different scanner types and MR protocols (GE 3D-SPGR and Siemens MP-RAGE). Reconstructing and aligning as before, we found the mean cross-scanner standard deviation in the thickness measures increased slightly over the within-platform case to 0.31 mm (0.23 mm with the same blurring kernel as before), suggesting that the measurements are relatively robust to differences in MR protocols and scanners. These results indicate that much of the variability in the cross-subject thickness measurements reflects true inter-subject differences, and that even focal abnormalities in cortical thickness may be detectable with these techniques.

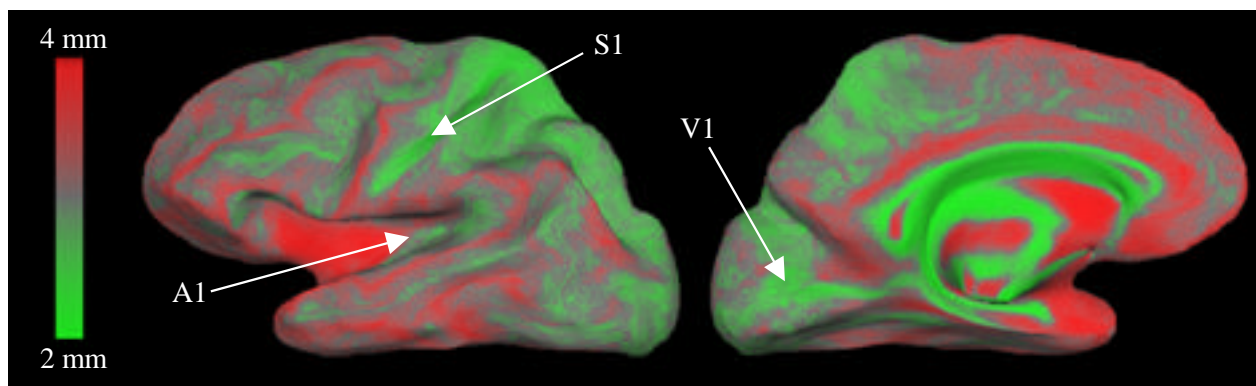


Figure 4. Average cortical thickness across thirty subjects, with primary auditory (A1), somatosensory (S1) and visual (V1) cortices indicated by the white arrows.

a gyral (or sulcal) patch in any other individual. Note that 100% alignment is not possible due to the fact that the topology of the folding patterns varies substantially across individuals, and thus no continuous bijection exists.

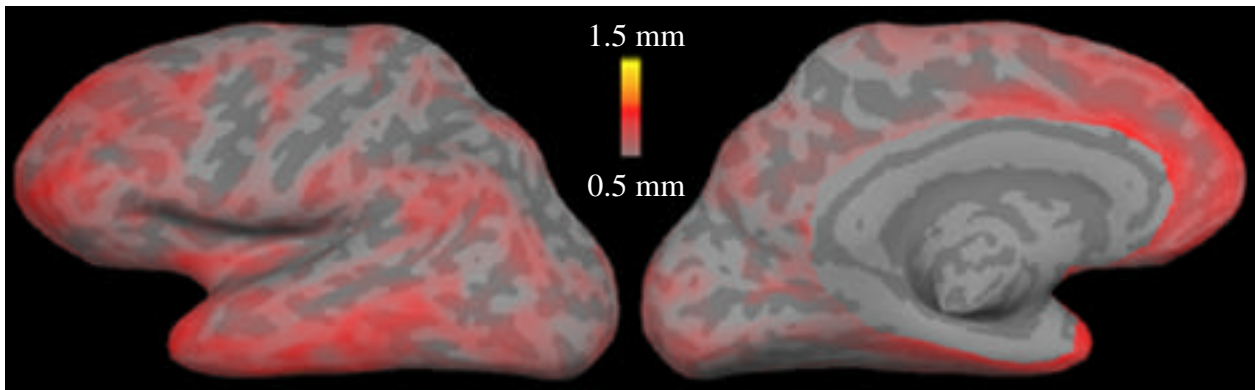


Figure 5. Map of the standard deviations of the thickness measurements across 30 subjects. Non-cortical regions have been excluded on the medial aspect of the surface.

Further validation was obtained by comparing the automated thickness measurements with manual measurements of cortical thickness from MRI data. A recent study, in which a trained anatomist used a jeweler’s eyepiece to estimate the thickness in 0.1 mm gradations from slices oriented perpendicular to the central sulcus, found that the thickness of the anterior and posterior banks of the sulcus differed substantially [20], in agreement with earlier postmortem results [2]. Specifically, the average thickness of the anterior bank of the central sulcus was found to be 2.69 mm, while the average thickness of the posterior bank was substantially less, averaging 1.81 mm, allowing the banks to be distinguished based solely on thickness. Figure 6 illustrates these manually measured findings, and compares them with the average thickness measured with our technique across the left hemispheres of the same 30 subjects. As can be seen, our measurements are in close agreement with the MR results, as well as earlier postmortem work that found the mean thickness of the anterior and posterior banks to be 2.7 mm and 1.7 mm respectively [39]. It is important to note here that these results validate both the accuracy of the thickness measurements and the precision of the inter-subject alignment in this region. That is, if the alignment procedure did not map anterior banks to anterior banks and posterior banks to posterior banks, the thick cortex on the anterior bank would be averaged with the thin cortex on the posterior bank, yielding no distinction between the two banks in the average.

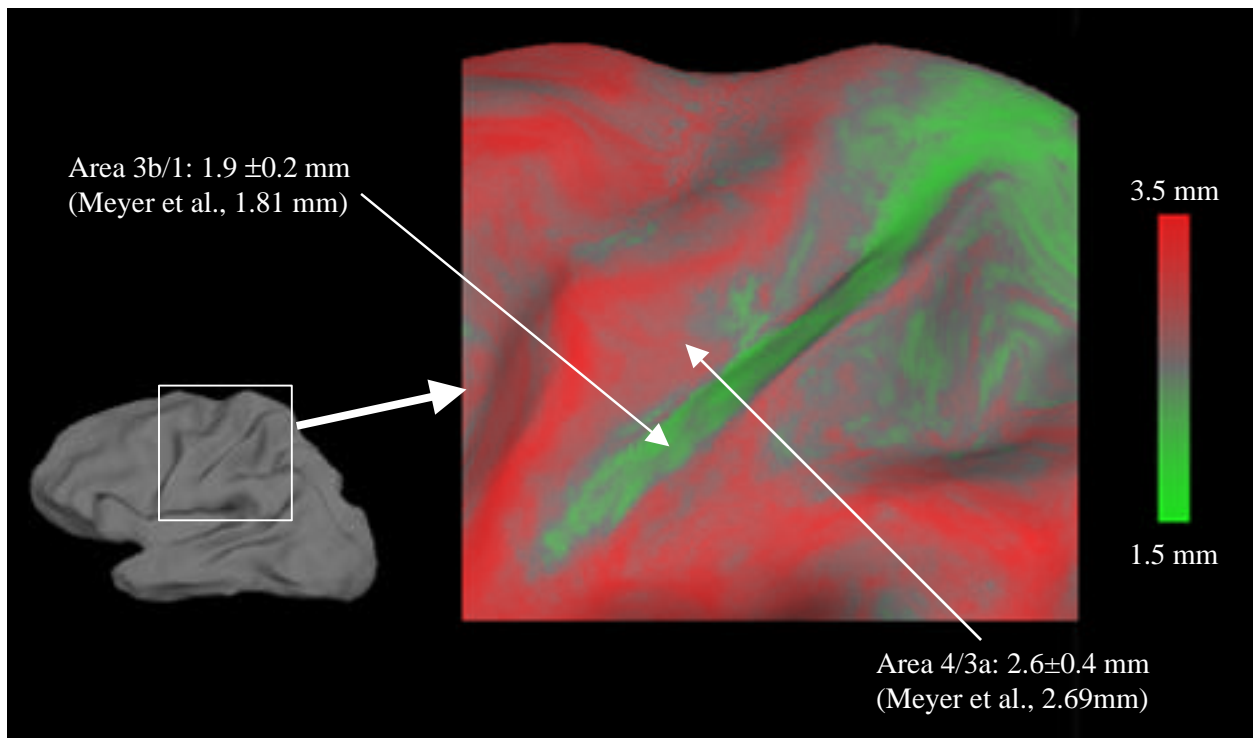


Figure 6. Average thickness of posterior (area 3b/1) and anterior (area 3a/4) banks of the central sulcus together with a comparison of manually measured published values.

Finally, a more quantitative and regionally specific comparison with postmortem findings was performed, the results of which are summarized in Table 1⁴. Note the excellent agreement between the overall average measured using the current procedure and the postmortem results. Further, the agreement in the regional measurements generated using the two techniques is quite good, with a maximum discrepancy of slightly more than $\frac{1}{2}$ mm. These differences may be accounted for by a number of factors such as individual variability, fixation effects, the precise location of the measurements, as well as MR artifacts.

Overall average	2.5 mm [2]	2.5 ± 0.7 mm
Lateral cortex	3.5 mm [2]	2.9 ± 0.3 mm
Medial cortex	2.7 mm [2]	2.4 ± 0.3 mm
Inferior cortex	3.0 mm [2]	2.7 ± 0.3 mm

Table 1. Comparison of reported postmortem thickness (column 2) with the automated methods outlined in this paper, averaged across 30 subjects (column 3). All ranges are standard deviations.

⁴ The measurements summarized in Table 1 (both ours and the published values) were all taken at the crowns of the gyri.

4. Conclusion.

The methods presented here provide highly accurate models of both the gray/white and the pial surfaces of the human cerebral cortex as a precursor to measuring the thickness of the cortical ribbon. The procedure for positioning these surfaces ensures smoothness without sacrificing accuracy in highly folded regions, resulting in a pair of surfaces with sub-millimeter accuracy. The thickness of the gray matter can then be easily computed at any point in the cortex as the shortest distance between the two surfaces. The comparison with published values indicates that the thickness measurements can accurately reflect sub-millimeter variations in the gray matter. This level of accuracy, in conjunction with the small standard deviations of the measurements across most of cortex, implies the ability to distinguish focal atrophy in small patient populations or even individuals. In addition, given the high within-subject test-retest reliability it should be possible to detect subtle localized changes in thickness over time in individual subjects, a capability that may prove important in studying the progression of a disease, as well as for assessing the efficacy of treatments.

The precision of the thickness measurements is, of course, constrained by the contrast-to-noise ratio and fidelity of the underlying MRI data. Although our studies indicate that the methods are relatively insensitive to the specifics of the MR imaging protocol and scanner, it should be noted that gray/white matter contrast varies across the cortex. In particular, primary sensory areas tend to have a high degree of myelination resulting in reduced contrast, in these regions. In order to obtain accurate measurements throughout the cortex, including these regions, sequences must be used that provide sufficient spatial resolution and T1 contrast.

In most morphological studies one wishes to compare average measures across groups (e.g. patients and controls). In order to carry out this type of comparison, some procedure must be used to relate the points in one cortical hemisphere with those in another. This is of importance as the ability to meaningfully assess the early progress of a number of diseases is limited by both the accuracy of the thickness measurements and the precision of the point correspondence across brains. The standard method of averaging human neuroimaging data [40] does not afford the anatomical specificity required to

make this type of subtle comparison. In contrast, using a high-resolution surface-based averaging technique that aligns cortical folding patterns [25], we have shown the ability to distinguish the opposing banks of the central sulcus based on variations in mean cortical thickness across a large number of individuals. This level of accuracy is critical for diagnostic purposes, as well as for furthering the understanding of intra-cortical and afferent functional connectivity patterns, as atrophy is frequently associated with a substantial decrease in a previously active set of connections.

The results presented in this study were achieved by combining a number of novel techniques. These include methods for constructing [22, 24] and transforming [23] models of the human cerebral cortex, as well as a means for using the pattern of cortical folding derived from these models to drive a high-resolution inter-subject alignment procedure [25]. These tools, as well as those for measuring cortical thickness and visualizing morphometric and functional properties of the cortex, are part of a freely available software package⁵. Furthermore, the pattern of cortical folds, in the form of mean curvature, Gaussian curvature, or average convexity, can be used to characterize geometric differences between populations in much the same manner as cortical thickness, a capability that may be useful in studying disorders associated with abnormalities in cortical folding patterns, such as polymicrogyria. The combination of these tools yields a set of powerful techniques for analyzing morphometric properties of the human cerebral cortex, with important applications in the study of the patterns of geometric changes associated with specific diseases, as well normal brain development and aging.

5. Acknowledgments.

This Human Brain Project/Neuroinformatics research is funded jointly by the National Institute of Neurological Disorders and Stroke, the National Institute of Mental Health and the National Cancer Institute (R01-NS39581). Further support was provided by the National Center for Research Resources (P41-RR14075 and R01-RR13609). We thank David Van Essen, Eric Halgren, Christophe Destrieux, David Salat and Arthur Liu for useful discussions about measuring cortical thickness, as well

⁵ The software can be downloaded from <http://www.nmr.mgh.harvard.edu/freesurfer>.

as for extensive work validating the proposed technique. We also thank Randy Buckner for providing data for testing the thickness measurement procedure, Kevin Teich for providing many useful graphical tools, and Diana Rosas and Eduard Kraft for helpful discussions regarding neurodegenerative disorders.

6. References.

1. Zilles, K., *Cortex*, in *The Human Nervous System*. 1990, Academic Press: San Diego, CA. p. 575-802.
2. von Economo, C., *The cytoarchitectonics of the human cerebral cortex*. 1929, London: Oxford University Press.
3. Brodmann, K., *Vergleichende Lokalisationslehre der Großhirnrinde in ihren Prinzipien dargestellt auf Grund des Zellenbaues*. 1909, Leipzig: Barth.
4. Leon, M.J.D., A.E. George, J. Golomb, C. Tarshish, A. Convit, A. Kuger, S.D. Santi, T. McRae, S.H. Ferris, B. Reisberg, C. Ince, H. Rusinek, M. Bobinski, B. Quinn, D.C. Miller, and H.M. Wisniewski, *Frequency of Hippocampal Formation Atrophy in Normal Aging and Alzheimer's Disease*. *Neurobiology of Aging*, 1997. **18**(1): p. 1-11.
5. Jack, C.R., R.C. Petersen, Y.C. Xu, S.C. Waring, P.C. O'Brien, E.G. Tangalos, G.E. Smith, R.J. Ivnik, and E. Kokmen, *Medial Temporal atrophy on MRI in normal aging and very mild Alzheimer's disease*. *Neurology*, 1997. **49**: p. 786-790.
6. Albert, M.S., *Cognitive and neurobiologic markers of early Alzheimer disease*. *Proceedings of the National Academy of Sciences*, 1996. **93**: p. 13547-13551.
7. Frisoni, G.B., A. Beltramello, C. Weiss, C. Geroldi, A. Bianchetti, and M. Trabucchi, *Linear Measures of Atrophy in Mild Alzheimer Disease*. *American Journal of Neuroradiology*, 1996. **17**: p. 913-923.
8. Grignon, Y., C. Duyckaerts, M. Bennechib, and J. Hauw, *Cytoarchitectonic alterations in the supramarginal gyrus of late onset Alzheimer's disease*. *Acta Neuropathologica (Berl)*, 1998. **4**: p. 395-406.

9. Double, K., G. Happiday, J. Dril, J. Harasty, K. Cullen, W.S. Brooks, H. Creasey, and G.A. Broe, *Topography of brain atrophy during normal aging and Alzheimer's disease*. *Neurobiology of Aging*, 1996. **17**: p. 513-521.
10. Rusinek, H., M. de Leon, A. George, L. Stylopoulos, R. Chandra, G. Smith, T. Rand, M. Mourino, and H. Kowalsky, *Alzheimer disease: measuring loss of cerebral grey matter with MR imaging*. *Radiology*, 1991. **178**: p. 109-114.
11. Kaye, J.A., T. Swihart, D. Howieson, A. Dame, M.M. Moore, T. Karnos, R. Camicioli, M. Ball, B. Oken, and G. Sexton, *Volume loss of the hippocampus and temporal lobe in health elderly persons destined to develop dementia*. *Neurology*, 1997. **48**: p. 1297-1304.
12. Vonsattel, J.P. and M. DiFiglia, *Huntington disease*. *Journal of Neuropathology and Experimental Neurology*, 1998. **57**(5): p. 369-84.
13. Halliday, G.M., D.A. McRitchie, V. Macdonald, K.L. Double, R.J. Trent, and E. McCusker, *Regional specificity of brain atrophy in Huntington's disease*. *Experimental Neurology*, 1998. **154**(2): p. 663-72.
14. Boeve, B., D. Maraganore, J. Parisi, J. Ahlskog, N. Graff-Radford, R. Caselli, D. Dickson, E. Kokmen, and R. Peterson, *Pathologic heterogeneity in clinically diagnosed corticobasal degeneration*. *Neurology*, 1999. **52**: p. 795-800.
15. Kiernan, J. and A. Hudson, *Frontal lobe atrophy in motor neuron diseases*. *Brain*, 1994. **117**: p. 747-757.
16. Zipursky, R.B., K.O. Lim, E.V. Sullivan, B.W. Brown, and A. Pfefferbaum, *Widespread Cerebral Gray Matter Volume Deficits in Schizophrenia*. *Archives of General Psychiatry*, 1992. **49**: p. 195-205.
17. Zipursky, R.B., E.K. Lambe, S. Kapur, and D.J. Mikulis, *Cerebral gray matter volume deficits in first episode psychosis*. *Archives of General Psychiatry*, 1997. **55**(6): p. 540-546.
18. Pfefferbaum, A. and L. Marsh, *Structural Brain Imaging in Schizophrenia*. *Clinical Neuroscience*, 1995. **3**: p. 105-111.

19. Kwon, J., R. McMarley, Y. Hirayasu, J. Anderson, I. Fischer, R. Kikinis, F. Jolesz, and M. Shenton, *Left planum temporale volume reduction in schizophrenia*. Archives of General Psychiatry, 1999. **56**: p. 142-148.
20. Meyer, J.R., S. Roychowdhury, E.J. Russell, C. Callahan, D. Gitelman, and M.M. Mesulam, *Location of the central sulcus via cortical thickness of the precentral and postcentral gyri on MR*. American Journal of Neuroradiology, 1996. **17**(9): p. 1699-1706.
21. Dale, A.M. and M.I. Sereno, *Improved localization of cortical activity by combining EEG and MEG with MRI cortical surface reconstruction: A linear approach*. Journal of Cognitive Neuroscience, 1993. **5**(2): p. 162-176.
22. Dale, A.M., B. Fischl, and M.I. Sereno, *Cortical Surface-Based Analysis I: Segmentation and Surface Reconstruction*. NeuroImage, 1999. **9**: p. 179-194.
23. Fischl, B., M.I. Sereno, and A.M. Dale, *Cortical Surface-Based Analysis II: Inflation, Flattening, a Surface-Based Coordinate System*. NeuroImage, 1999. **9**: p. 195-207.
24. Fischl, B., A. Liu, and A.M. Dale, *Automated Manifold Surgery: Constructing Geometrically Accurate and Topologically Correct Models of the Human Cerebral Cortex*. IEEE Transactions on Medical Imaging., 1999: p. Submitted.
25. Fischl, B., M.I. Sereno, R.B.H. Tootell, and A.M. Dale, *High-resolution inter-subject averaging and a coordinate system for the cortical surface*. Human Brain Mapping, 1999. **8**(4): p. 272-284.
26. Terzopoulos, D. and K. Fleischer, *Deformable models*. The Visual Computer, 1988. **4**(6): p. 306-331.
27. MacDonald, D., *A Method for Identifying Geometrically Simple Surfaces from Three Dimensional Images*, in *Montreal Neurological Institute*. 1998, McGill University: Montreal.
28. Davatzikos, C. and R.N. Bryan, *Using a Deformable Surface Model to Obtain a Shape Representation of the Cortex*. IEEE Trans. on Medical Imaging, 1996. **15**: p. 785-795.
29. Kaas, M., A. Witkin, and D. Terzopoulos, *Snakes: Active contour models*. International Journal of Computer Vision, 1988. **1**: p. 321-331.

30. Yuille, A.L., *Deformable Templates for Face Recognition*. Journal of Cognitive Neuroscience, 1991. **3**(1): p. 59-70.
31. Christensen, G.E., R.D. Rabbitt, and M.I. Miller, *Deformable Templates Using Large Deformation Kinematics*. IEEE Transactions on Image Processing, 1996. **5**(10): p. 1435.
32. Thompson, P.M. and A.W. Toga, *A surface-based technique for warping 3-dimensional images of the brain*. IEEE Transactions on Medical Imaging, 1996. **15**(4): p. 1-16.
33. McInerney, T. and D. Terzopoulos, *Deformable Models in Medical Image Analysis: A Survey*. Medical Image Analysis, 1996. **1**(2).
34. Burt, P.J. and E.H. Adelson, *The Laplacian pyramid as a compact image code*. IEEE Transactions on Communications, 1983. **9**(4): p. 532-540.
35. Sethian, J.A., *Level Set Methods. Evolving Interfaces in Geometry, Fluid Mechanics, Computer Vision, and Materials Science*. 1996, Cambridge: Cambridge University Press.
36. Sethian, J.A., *Numerical Algorithms for propagating interfaces: Hamilton-Jacobi equations and conservation laws*. Journal of Differential Geometry, 1990. **31**: p. 131-161.
37. Press, W.H., S.A. Teukolsky, W.T. Vetterling, and B.P. Flannery, *Numerical Recipes in C*. Second ed. 1994, Cambridge: Cambridge University Press.
38. Möller, T., *A Fast Triangle-Triangle Intersection Test*. Journal of Graphics Tools, 1997. **2**(2): p. 25-30.
39. Sholl, D.A., *The Organization of the Cerebral Cortex*. 1956, New York: John Wiley & Sons, Inc.
40. Talairach, J. and P. Tournoux, *Co-Planar Stereotaxic Atlas of the Human Brain*. 1988, New York: Thieme Medical Publishers.